Magnetic Circular Dichroism of Naphthalene Derivatives: A Coupled Cluster Singles and Approximate Doubles and Time-Dependent Density Functional Theory Study

S. Ghidinelli,[*,†] G. Longhi,[†] S. Abbate,[†] C. Hättig,[‡] and S. Coriani[*,¶]

†*Department of Molecular and Translational Medicine, Università degli Studi di Brescia, Viale Europa 11, 25123 Brescia, Italy.*

‡*Arbeitsgruppe Quantenchemie, Ruhr-Universität Bochum, D-44780, Germany*

¶*DTU Chemistry, Technical University of Denmark, Kemitorvet Bldg 207, DK-2800 Kongens Lyngby, Denmark*

E-mail: s.ghidinelli001@unibs.it; soco@kemi.dtu.dk

Abstract

The UV-Vis absorption and Magnetic Circular Dichroism spectra of naphthalene and some of its derivatives have been simulated at the Coupled Cluster Singles and Approximate Doubles (CC2) level of theory, and at the Time-Dependent Density Functional Theory level (TD-DFT) using the B3LYP and CAM-B3LYP functionals. DFT and CC2 predict in general opposite energetic ordering of the L_b and L_a transitions (in gas phase), as previously observed in adenine. The CC2 simulations of UV and MCD spectra show the best agreement with the experimental data. Analysis of the Cartesian components of the electric dipole transition strengths and the magnetic dipole transition moment between the excited states have been considered in the interpretation of the electronic transitions and the Faraday $\mathcal{B}$ term inversion among the naphthalene derivatives.

Introduction

The photoabsorption spectrum of naphthalene (and other polycyclic aromatic hydrocarbons in general) has been extensively investigated with several spectroscopic techniques, comprising Magnetic Circular Dichroism (MCD) spectroscopy. It has been shown that MCD spectroscopy is complementary to UV-Vis absorption spectroscopy, offering a better sensitivity to distinguish electronic transitions.[1] Foss and McCarville[2,3] observed a correlation between the sign of the Faraday $\mathcal{B}$ term and the direction of the electric transition dipole moment in the MCD spectra of toluene, naphthalene, anthracene, and tetracene. Further theoretical advancements in understanding the MCD response of polycyclic aromatic hydrocarbons were reported by Stephens[4] and Larkindale.[5]

In 1978, Michl published a series of papers where he proposed some general rules for a qualitative interpretation of the MCD spectra of (4N+2)-electron [n]annulene (where N is the number of π-electrons).[6–8] According to the nomenclature proposed by Platt,[9] the first four excited states are labelled as L_b, L_a, B_b, and B_a. On the basis of the π-electron perimeter

model, Michl was able to predict the sign of Faraday $\mathcal{A}$ and $\mathcal{B}$ terms for the bands given by the transitions from the ground state to the L and B states. Even though, in Michl's approach, only $\pi\pi^*$ mixing was considered for the evaluation of the $\mathcal{B}$-terms, the predicted results showed a good agreement with the experimental data (for this type of molecule, contributions from the magnetic $n\pi^*$–$\pi\pi^*$ mixing on the MCD signals are negligible).[10] This approach was also found to be useful for rationalizing contributions from substituents with inductive and mesomeric effects on the π-electron system by estimating the perturbation caused to HOMO and LUMO levels.[10] It was previously pointed out that the prediction of the correct energy ordering of the first two transitions, L_b and L_a, is not always obtained by simple TD-DFT calculations[11–13] unless a careful choice of functional is made.[14] Analogous problems have been found in substituted naphthalenes.[15] In this context, Coupled Cluster (CC) calculations have been reported, showing a significant improvement in the accurate prediction of L_b and L_a transitions.[11,15,16] Here, we present a Coupled Cluster Singles and approximate Doubles (CC2) and TD-DFT study of the absorption and MCD spectra of naphthalene and three mesomeric derivatives and compare them with the experimental data and with previous interpretations.

Computational methodology and details

The ground state geometries of the molecules reported in Figure 1 were optimized, in vacuo, at the CC2 level of theory using the aug-cc-pVDZ[17] basis set. The excitation energies, oscillator strengths and Faraday $\mathcal{B}$ terms were calculated within the response function formalism[16,18–21] at the CC2 level of theory with the resolution-of-the-identity (RI) approximation,[16] as implemented in Turbomole.[22,23] For the CC2 calculations the aug-cc-pVDZ orbital basis was used in combination with the corresponding optimized auxiliary basis set.[24] The excitation energies, oscillator strengths and Faraday $\mathcal{B}$ terms were also computed within the TD-DFT formalism,[18,20,25,26] adopting the B3LYP[27] and CAM-B3LYP[28] functionals and the

aug-cc-pVDZ basis set. The TD-DFT calculations were performed using the Dalton code.[29] A Lorentzian lineshape-function was chosen for the broadening of the MCD and absorption spectra (FWHM $\gamma = 1000$ cm^{-1}).[16,30] Experimental data have been re-digitized[31] and adapted from the work of Michl and coworkers.[10] For ease of comparison, a vertical translation has been applied to all experimental spectra, so that they do not overlap with the computed ones.

A characterization (composition and assignments) of the relevant excited states for naphthalene and its derivatives on the basis of CC2 Natural Transition Orbitals (NTO) is shown in Figure 2. Consistent with previous work,[14,32–34] the L_b excited state involves the HOMO-1 $\rightarrow$ LUMO and HOMO $\rightarrow$ LUMO+1 transitions with similar weights. The L_a transition, on the other hand, is dominated by HOMO $\rightarrow$ LUMO component.

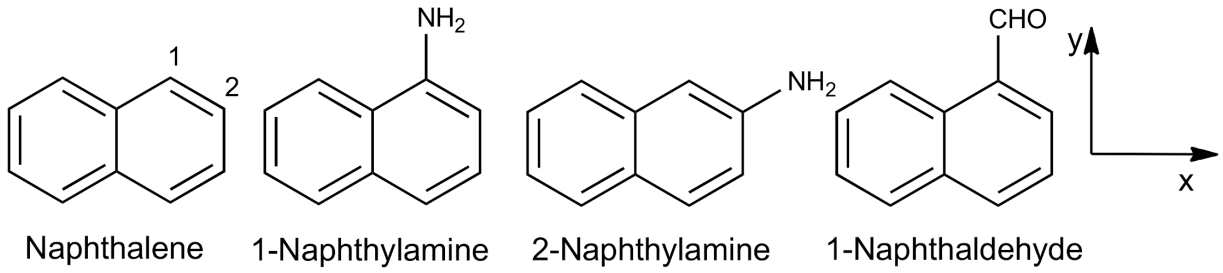

Figure 1: Structures of naphthalene and naphthalene derivatives. As indicated, the molecular plane is xy.

Results and discussion

In Table 1, the computed results of naphthalene at TD-DFT and CC2 levels of theory are collected. The calculated MCD and absorption spectra obtained for naphthalene are depicted in Figure 3, and compared with the corresponding experimental data.[10,35] The computed spectra have been shifted on the energy axis to align them to the experimental B band.

The experimental spectra of naphthalene, both UV and MCD, are characterized by vi-

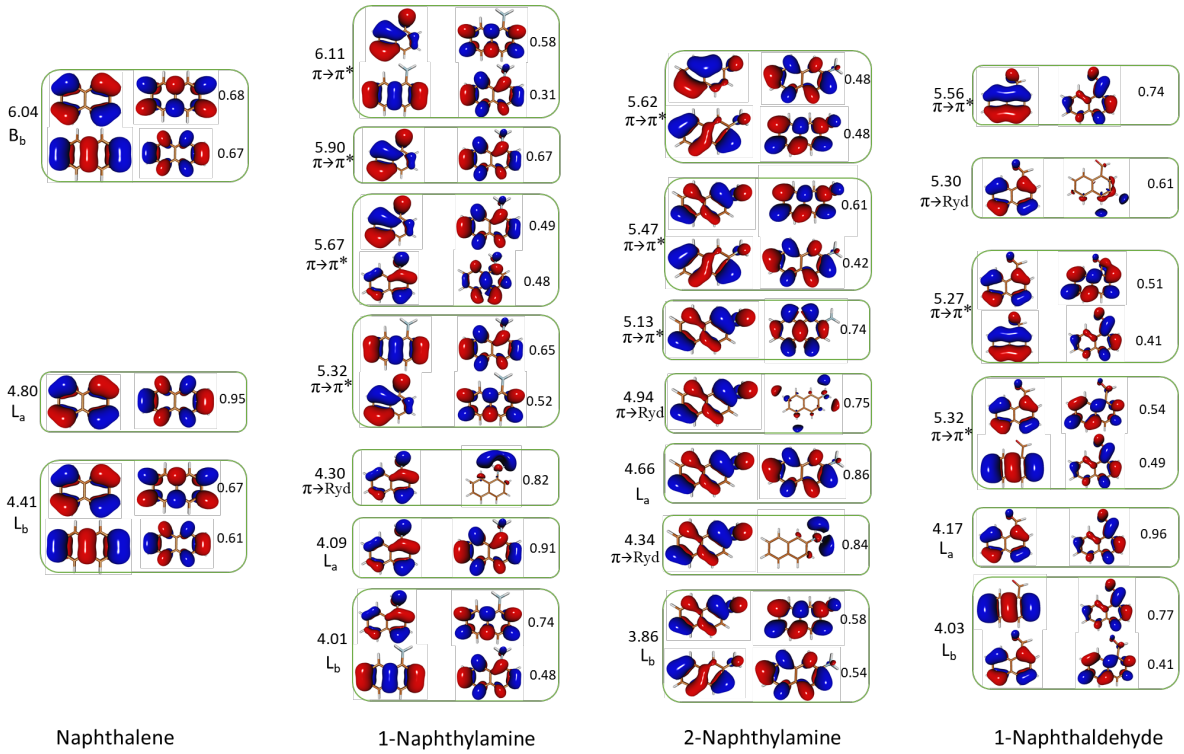

Figure 2: RI-CC2 calculated vertical excitation energies with the corresponding Natural Transition Orbital (NTO) composition and assignments for naphthalene and its derivatives. Pairs of occupied and virtual NTOs are given next to each other, with the occupied NTO on the left. If more than one NTO pair contribute substantially, the NTO pairs are stacked on the top of each other. The numbers of the right of the NTO pairs indicate their weights in the eigenvector.

bronic components.[36–38] Looking at the experimental UV, reproduced in the bottom panel of Fig. 3, the first transition (around 3.8-3.9 eV) has near zero strength and is almost all vibronic. It has been assigned to L_b. The second transition (roughly centered at 4.6 eV) has higher strength and it has been attributed to L_a. The strongest UV band is peaked at 5.6 eV and is assigned to B_b. For naphthalene and substituted naphthalene, the L_b state is lower in energy than the L_a state, both in the gas phase as well as in nonpolar/weakly polar solvents.[9,39–43] The CC2 calculations yield the correct energetic ordering,[11] $L_b < L_a$, for the first two transitions of naphthalene with a separation of 0.4 eV. The CAM-B3LYP calculations also correctly reproduce the energetic order of L_b and L_a,[34] but the separation between the two transition is only 0.04 eV. The B3LYP functional gives the inverted ordering, i.e. L_a at lower energy than L_b, as already discussed in previous works.[11–13,34] According to previous works,[44–46] the transition moment of L_b is directed along the long axis of the molecule (x axis in Figure 1). The transition moment of L_a is instead directed along the short axis (y axis in Figure 1). Our results are consistent with these studies.

The simulated UV absorption spectrum at the CC2 level is in good agreement with the experimental one and is consistent with the calculated spectra reported in previous studies.[38,47,48] Note that when simulating the spectra, we have scaled the intensities by the same factors as in experiment in Fig. 3—that is, a factor 10 for L_a and a factor 24 for L_b. B3LYP also yields two bands in the UV spectrum, but the L_a band is much more separated from the B_b band and moves in the frequency region experimentally attributed to the L_b band.

Both CC2 and TD-DFT yield a negative $\mathcal{B}$ term for the L_b band and a positive $\mathcal{B}$ term for the L_a band. As the $\mathcal{B}$ term of L_a is larger (roughly one order of magnitude for CC2 and B3LYP, and a factor 2 for CAM-B3LYP), it prevails in the MCD response in the spectral regions of the L states. The B_b state yields the largest (negative) MCD band. The MCD calculations thus reproduce the sign and the relative intensities of the experimental MCD bands, even though the vibronic effects are not included. A vibrational study of the MCD

bands of naphthalene is reported in Ref. 38. It is worth noting that the inverted order of the L_b and L_a transitions with the B3LYP functional is not accompanied by a sign inversion of the associated $\mathcal{B}$ terms, as otherwise observed in adenine.[16,49] Sign inversion of the $\mathcal{B}$ terms of two energetically close states upon switching of their order happens if their $\mathcal{B}$ terms are dominated by the contribution from the magnetic dipole transition moments between them

$$\mathcal{B}(0 \to 1) \approx \epsilon_{\alpha\beta\gamma} \frac{m_\alpha^{12} d_\beta^{01} d_\gamma^{20}}{\omega_2 - \omega_1} = -\epsilon_{\alpha\beta\gamma} \frac{m_\alpha^{21} d_\beta^{02} d_\gamma^{10}}{\omega_1 - \omega_2} \approx -\mathcal{B}(0 \to 2) \tag{1}$$

In this case, the $\mathcal{B}$ terms of these two states give rise to a bisignate feature in the MCD spectrum which is invariant under inversion of the order of the two states. For naphthalene, the magnetic dipole transition moment between the L_b and L_a states contributes at the CC2 level with, respectively, -1.6 and $+1.6$ to their $\mathcal{B}$ terms. For L_b another significant contribution of $+0.4$ arises from the coupling to the B_a state, and for L_a the $\mathcal{B}$ term is dominated by the much larger contribution from the coupling to the B_b states which contributes with $\approx +8$. Because of the small ground to excited state electric transition strength of L_a, the couplings to the B and higher-lying states are thus (more) important than the L_a and L_b coupling. This explains why for naphthalene the $\mathcal{B}$ terms of the L states do not flip signs when their order switches from CC2 or CAM-B3LYP to B3LYP. Thus, the inverted state ordering has little effect on the appearance of the simulated MCD spectrum and the contribution of the positive $\mathcal{B}$ term (negative band) of L_a is predominant in any case.

The introduction of a substituent in the parent molecule brings changes in the chemical and physico-chemical properties of the aromatic system, such as reactivity, electronic and magnetic properties.[50–53] Such changes are dependent on the nature and the position of the substituent.[50,52–54] Substitutions which affect the delocalization of the π electrons in a conjugated orbital system are referred to as mesomeric (M).[54] If the substituent carries an empty antibonding orbital, as in the case of the CHO group, it results in an electron-withdrawing (negative) mesomeric effect ($-$M).[8,54] If the substituent carries a filled bonding or non-

Table 1: Naphthalene. Calculated excitation energies ΔE_j (eV), oscillator strengths (f) with the Cartesian component of the transition strength (S) and Faraday $\mathcal{B}$ term (a.u.). Basis set aug-cc-pVDZ.

ΔE_j	$f(0 \to j)$	$\mathcal{B}(0 \to j)$
	RI-CC2	
4.41 (L_b)	4×10^{-5} (S_x=4×10^{-4}; S_y=0)	−1.2
4.80 (L_a)	0.08 (S_x=0; S_y=0.66)	13.8
6.04 (B_b)	1.44 (S_x=9.7; S_y=0)	107.9
6.14	0.018 (S_z=0.12)	−9.3
6.37	0.26 (S_x=0; S_y=1.7)	−95.2
6.41	0.019 (S_z=0.12)	10.6
	B3LYP	
4.30 (L_a)	0.05 (S_x=0; S_y=0.51)	8.0
4.40 (L_b)	3×10^{-5} (S_x=0.004; S_y=0)	−1.3
5.80 (B_b)	1.25 (S_x=8.8; S_y=0)	123.3
5.91	0.02 (S_z=0.12)	−2.5
6.01	0.18 (S_x=0; S_y=1.21)	−106.8
6.04	0.01 (S_z=0.1)	6.1
	CAM-B3LYP	
4.55 (L_b)	5×10^{-6} (S_x=4×10^{-5}; S_y=0)	−4.6
4.59 (L_a)	0.07 (S_x=0; S_y=0.6)	8.5
5.98 (B_b)	1.32 (S_x=9.06; S_y=0)	121.8
6.25	0.25 (S_x=0; S_y=1.29)	−100.6
6.38	0.03 (S_z=0.18)	−6.9
6.59	0.01 (S_z=0.08)	1.8

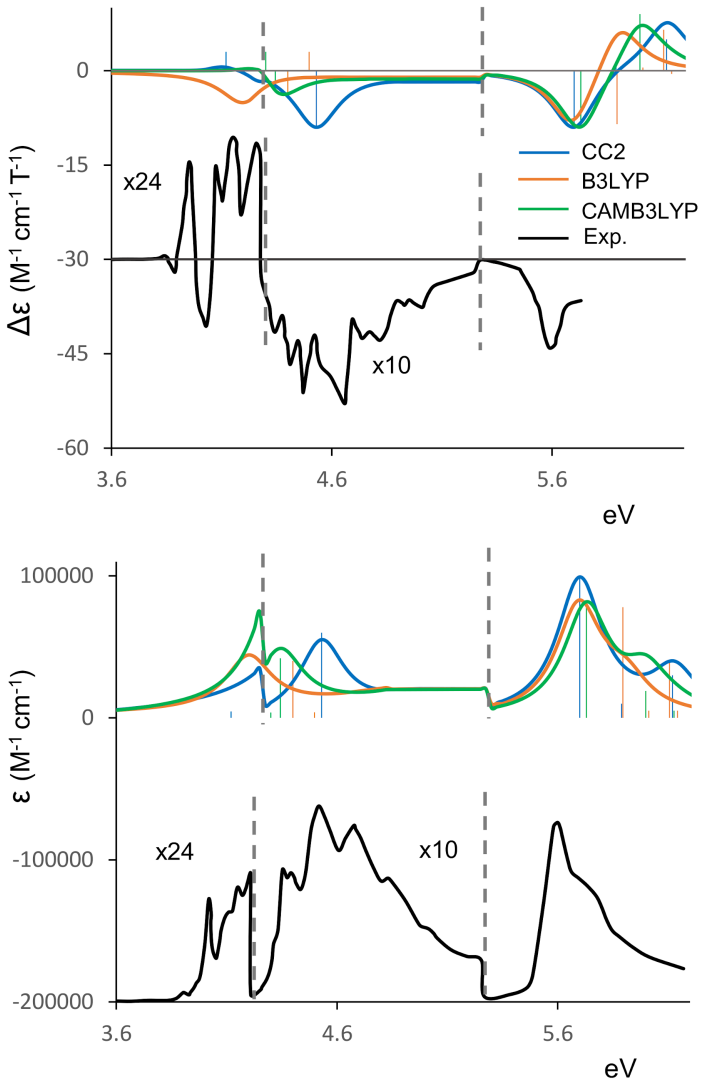

Figure 3: Naphthalene. Experimental[35] (recorded in cyclohexane, black lines) and calculated UV absorption (*bottom*) and MCD (*top*) spectra. A vertical translation was applied on the experimental spectra. The computed spectra have been shifted to align them with the experimental B_b peak at 5.6 eV. The CC2 and CAM-B3LYP spectra have been enhanced by the same scaling factors as experiment in the different frequency regions. For a coherent comparison, the B3LYP sticks of L_a have been scaled by 10 and those of L_b by 24. The sticks in the MCD spectrum correspond to $-\mathcal{B}$ values, according to the standard MCD convention. Horizontal shift applied: -0.25 eV for CC2 and CAM-B3LYP results, $+0.2$ eV for B3LYP results.

bonding orbital of π-symmetry, as in the case of amino groups, the result is an electrons donation, corresponding in an electron-donating (positive) mesomeric effect (+M).[8,54]

For naphthalene, as for other acenes, the substitution lowers the symmetry. Together,

this can change the state ordering and the weights with which orbital transitions contribute to a transition.[12,13] UV-Vis and MCD spectra for 1-Naphthylamine and 1-Naphthylaldehyde are shown in Figure 4 and 5, respectively. The spectra for 2-Naphthylamine are shown in Figure 6. The computed spectra were obtained from the energies, oscillator strengths and $\mathcal{B}$ terms tabulated in Tables 2, 3 and 4. As observed for naphthalene, the CC2 method predicts the L_b transition at lower energy than L_a for all three substituted naphthalenes. Both, B3LYP and CAM-B3LYP, on the other hand, give $L_a < L_b$ for the three substituted cases,[15] see Tables 2, 4 and 3.

Table 2: 1-Naphthylamine. Calculated excitation energies ΔE_j (eV), oscillator strengths (f) with the Cartesian component of the transition strength (S) and Faraday $\mathcal{B}$ term (a.u). Basis set aug-cc-pVDZ.

ΔE_j	$f(0 \rightarrow j)$	$\mathcal{B}(0 \rightarrow j)$
	RI-CC2	
4.01 (L_b)	0.03 (S_x=0.27; S_y=4×10^{-4})	155.8
4.09 (L_a)	0.10 (S_x=0.01; S_y=1.08)	−146.9
4.30	0.01 (S_z=0.09)	0.6
5.32	0.38 (S_x=2.2; S_y=0.02)	46.2
5.67	0.04 (S_x=0.009; S_y=0.3)	−19.2
5.90	0.03 (S_x=0.03; S_y=0.12)	35.1
6.11	0.62 (S_x=3.1; S_y=0.03)	29.3
	B3LYP	
3.69 (L_a)	0.07 (S_x=0.13; S_y=0.67)	109.2
4.05 (L_b)	0.05 (S_x=0.45; S_y=0.06)	−116.8
4.16	0.005 (S_z=0.05)	1.6
5.18	0.23 (S_x=1.37; S_y=0.41)	99.5
5.41	0.17 (S_x=1.28; S_y=0.001)	−42.4
5.94	0.03 (S_x=0.09; S_y=0.15)	62.3
6.01	0.82 (S_x=4.1; S_y=0.11)	5.4
	CAM-B3LYP	
4.01 (L_a)	0.11 (S_x=0.16; S_y=0.92)	84.3
4.26 (L_b)	0.05 (S_x=0.46; S_y=0.03)	−77.8
4.51	0.006 (S_z=0.05)	0.8
5.40	0.49 (S_x=3.0; S_y=0.4)	77.2
5.67	0.01 (S_x=0.4; S_y=0.09)	−30.7
5.76	0.004 (S_x=0.06; S_y=0.04)	100.4
5.99	0.63 (S_x=3.7; S_y=0.1)	30.2

We start with the analysis of the effect of the naphthalene derivatives substituted in

Table 3: 1-Naphthaldehyde. Calculated excitation energies ΔE_j (eV), oscillator strengths (f) with the Cartesian component of the transition strength (S), and Faraday $\mathcal{B}$ term (a.u.). Basis set aug-cc-pVDZ.

ΔE_j	$f(0 \rightarrow j)$	$\mathcal{B}(0 \rightarrow j)$
	RI-CC2	
4.03 (L_b)	0.02 (S_x=0.16; S_y=0.09)	−90.4
4.17 (L_a)	0.15 (S_x=0.1; S_y=1.4)	79.8
5.12	0.36 (S_x=2.8; S_y=0.001)	31.1
5.27	0.02 (S_x=0.05; S_y=0.02)	−70.4
5.30	0.01 (S_z=0.08)	0.4
5.56	0.11 (S_x=0.15; S_y=0.85)	80.9
	B3LYP	
3.51 (L_a)	0.11 (S_x=0.29; S_y=0.90)	−39.1
3.88 (L_b)	0.03 (S_x=0.12; S_y=0.15)	69.6
4.76	0.28 (S_x=0.72; S_y=1.02)	89.9
4.81	0.03 (S_x=0.001; S_y=0.26)	−107.
5.12	0.01 (S_z=0.001)	0.3
5.27	0.10 (S_x=0.42; S_y=0.37)	75.6
	CAM-B3LYP	
4.14 (L_a)	0.15 (S_x=0.4; S_y=1.12)	−70.1
4.33 (L_b)	0.02 (S_x=0.08; S_y=0.13)	77.6
5.40	0.38 (S_x=1.01; S_y=1.77)	−72.5
5.61	0.01 (S_x=0.62; S_y=0.14)	83.0
5.74	0.06 (S_z=0.005)	20.7
6.10	0.11 (S_x=0.86; S_y=0.07)	10.1

position 1, see Figures 4 and 5 and Tables 2 and 3.

The two different substituents significantly affect the electronic transitions of the two naphthalene derivatives. Experimentally, both amino and CHO group substitutions in position 1 move the L_a transition to lower energy with respect to the unsubstituted naphthalene, whereas the L_b transition is almost unchanged in energy, which results in an overlap of L_b and L_a bands in the 1-substituted naphthalene molecules.[40,55] For 1-Naphthylamine, the transition moments of L_b and L_a are polarized almost perpendicular to each other, as in the unsubstituted naphthalene, whereas in 1-Naphthaldehyde the angle between the two transition moments is significantly smaller (around 62 degree), mostly due to the rotation of the L_b transition moment (see Table 3).

The above trends are generally confirmed by the CC2 results: in 1-Naphthylamine, the

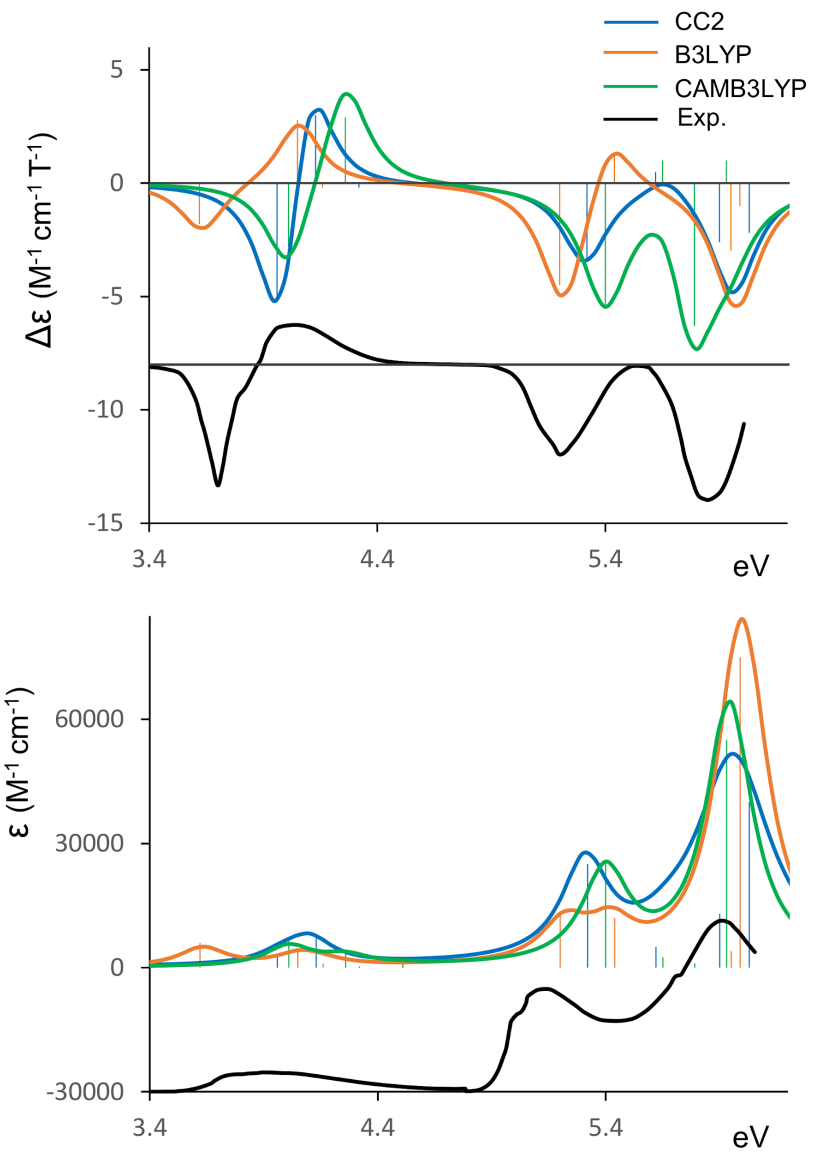

Figure 4: 1-Naphthylamine. Experimental[10] (recorded in acetonitrile, black lines) and calculated UV absorption (*bottom*) and MCD (*top*) spectra. A vertical translation was applied on the experimental spectra.

L_a excitation moves down by ≈0.7 eV to 4.09 eV (vs 4.80 eV in naphthalene), whereas the L_b transition moves by a more modest ≈0.4 eV to 4.01 eV, so the two transitions almost overlap. In 1-Naphthaldehyde, L_b moves by ≈ 0.4eV and L_a by 0.63 eV to the red, so their separation is ≈0.15 eV.

The two DFT functionals do not reflect the above trends: according to both the B3LYP

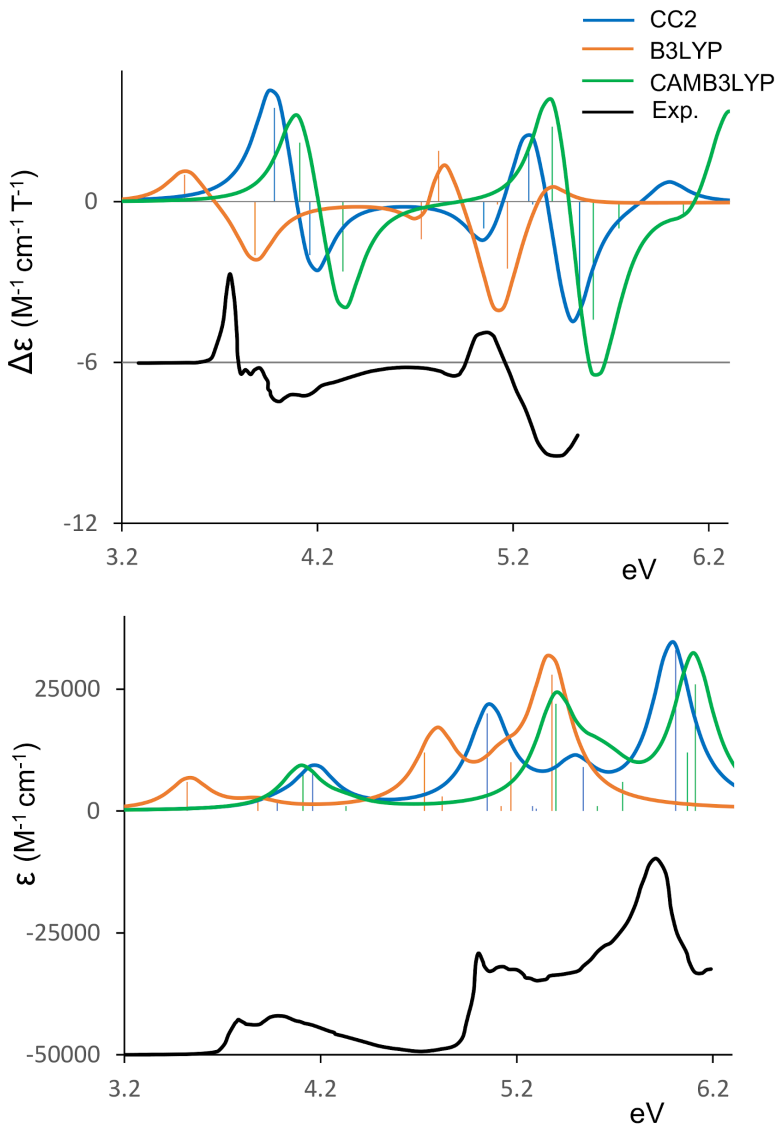

Figure 5: 1-Naphthaldehyde. Experimental[10] (recorded in cyclohexane, black lines) and calculated UV absorption (*bottom*) and MCD (*top*) and spectra. A vertical translation was applied on the experimental spectra.

and the CAM-B3LYP calculations, the L_a and L_b states of 1-Naphthylamine move to lower energy compared to naphthalene, but their splittings also increases. A similar behaviour is found for the 1-Naphthaldehyde case.

MCD spectroscopy magnifies the differences compared to UV absorption due to the possibility to observe changes in sign in the bands. It was observed by Michl and coworkers that the amino substituent leads to a positive $\mathcal{B}$ term for the L_b transition and a negative

$\mathcal{B}$ term for the L_a transition.[10] Opposite behavior was observed for the MCD spectrum of 1-Naphthylaldehyde, where a negative $\mathcal{B}$ term was associated with the L_b transition and a positive $\mathcal{B}$ term was associated with the L_a one.[10] As a consequence, characteristic, and reasonably well resolved, asymmetric double signed spectral patterns emerge in correspondence of the two states L_a and L_b.

The CC2 results are in line with these observations. As pointed out earlier, the two DFT functionals yield reverse order of the L_a and L_b transitions compared to CC2. Yet, the L_a transitions always have positive $\mathcal{B}$ term for the amines and negative for the aldehyde, and vice-versa for the L_b transitions. In other words, the TD-DFT L_a and L_b transitions have reversed energetic order compared to CC2, as well as opposite sign of the $\mathcal{B}$ terms, as also observed in gas phase for adenine.[16] For the substituted naphthalenes, both L states have sizeable oscillator strengths and, thus, the coupling between the two states becomes much more important for their $\mathcal{B}$ terms and leads to bisignate profile which is invariant under inversion of the states' ordering. As a consequence, the appearance of a double signed L_a/L_b band is reproduced by the two TD-DFT functionals as well. It has been observed that the polarization of the transition moment for L_b and L_a bands of a substituted naphthalene varies depending on the mixing with other allowed transitions.[40,56]

Moving towards higher energies, several transitions contribute to the spectral region characteristic of the B bands. In 1-Naphthylamine, both CC2 and CAM-B3LYP yield two relatively intense transitions plus two weaker ones, whereas B3LYP has three relatively intense transitions plus a weaker one. The sign pattern of the corresponding $\mathcal{B}$ terms is the same in all three methods, but the magnitudes of the $\mathcal{B}$ terms themselves are quite different. As a consequence, the B3LYP MCD spectrum in this region shows a positive band that is absent in the experiment. The CC2 MCD spectrum is in excellent agreement with the experimental one. In 1-Naphthaldehyde, all three electronic structure methods yield in absorption two intense and two weak electronic transitions, but with different sign patterns as far as the $\mathcal{B}$ terms are concerned. The $\mathcal{B}$ term of the first B band is positive both for

CC2 and B3LYP, followed by a larger negative one. The opposite occurs for CAM-B3LYP. As a consequence, CAM-B3LYP does not reproduce the MCD negative/positive/negative spectral pattern in the experimental MCD spectrum in this frequency region.

Considering the case of the amino group as substituent, we compare the effect of substitution at 1 and 2 positions. The substitution in 2 position shifts the L_b transition to lower energy with respect to both naphthalene and 1-Naphthylamine, resulting in well-separated L_b and L_a bands.[40,55] In 2-Naphthylamine, the transition moment of L_b is not directed parallel the long-axis of the molecule, but it is rotated toward the short-axis[10,56] (see Table 4). The MCD spectrum of 2-Naphthylamine (Figure 6) shows a relevant difference from the MCD spectrum of 1-Naphthylamine (Figure 4): the $\mathcal{B}$ term of the L_b transition of 2-Naphthylamine is significantly weaker (about one-tenth) than the corresponding one of 1-Naphthylamine. The $\mathcal{B}$ term of the L_a transition of 2-Naphthylamine is weaker and opposite in sign with respect to the corresponding one in 1-Naphthylamine. Other differences are also present for the transitions at higher energy (see Table 2 and Table 4). As for the previous cases, the CC2 spectra are in best agreement with the experimental spectra.

Conclusion

In conclusion, CC2 provides a good representation of all four aromatic systems, well reproducing their electronic transitions as UV absorption, confirmed by the accurate prediction of their MCD response. All trends upon introduction of a substitutent in the naphthalene parent molecule discussed by Michl and coworkers[10] are confirmed by our CC2 calculations. On the other hand, both TD-B3LYP and TD-CAM-B3LYP fail to correctly reproduce some of the UV and MCD spectral features, and offer discording characterizations of the underlying electronic transitions. We attribute these problems to different mixing of the excited states induced by the substitutions which are not accurately reproduced by TD-DFT because of larger errors in the relative energies for different orbital transitions.

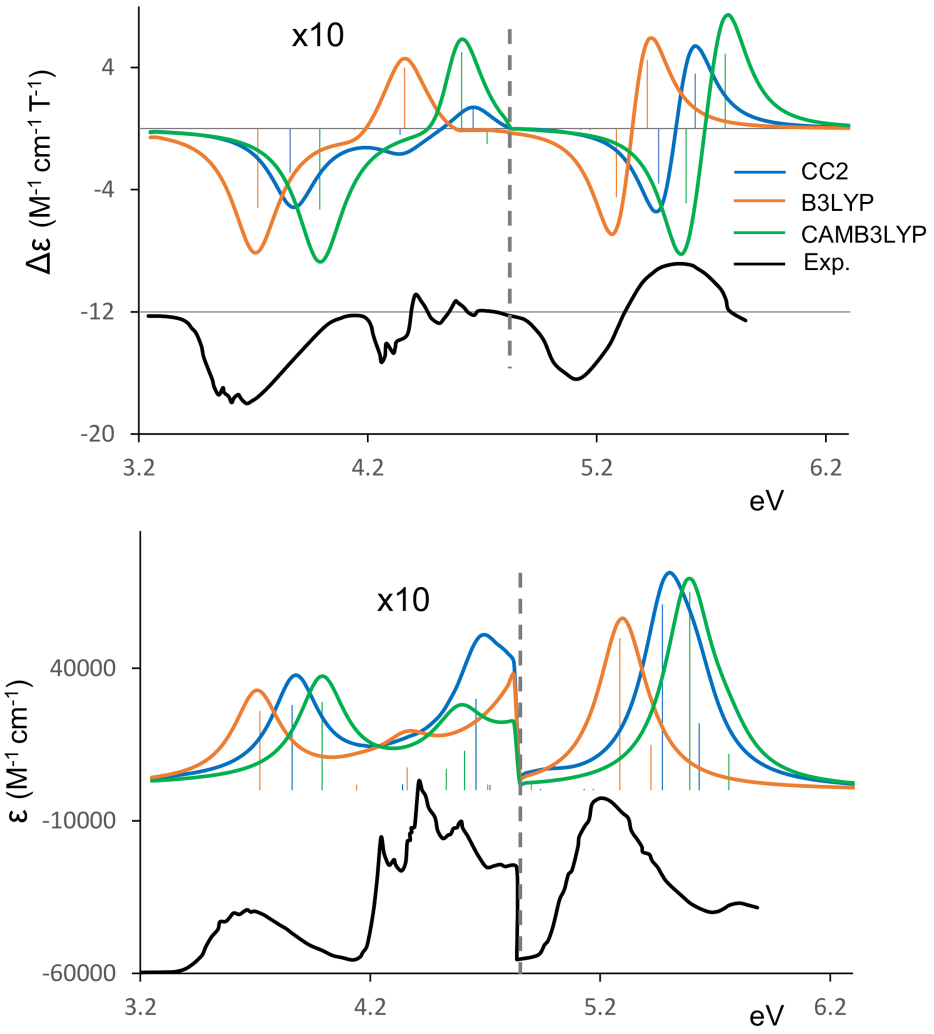

Figure 6: 2-Naphthylamine. Experimental (recorded in acetonitrile, black line) and calculated UV absorption (*bottom*) and MCD (*top*) spectra. A vertical translation was applied on the experimental spectra. The CC2 and TD-DFT calculations spectra have been enhanced by the same scaling factor as experiment.

Table 4: 2-Naphthylamine. Calculated excitation energies ΔE_j (eV), oscillator strengths (f) with the Cartesian component of the transition strength (S) and Faraday $\mathcal{B}$ term (a.u). Basis set aug-cc-pVDZ.

ΔE_j	$f(0 \rightarrow j)$	$\mathcal{B}(0 \rightarrow j)$
	RI-CC2	
3.86 (L_b)	0.051 (S_x=0.3; S_y=0.38)	16.1
4.34	0.005 (S_z=0.04)	1.5
4.66 (L_a)	0.055 (S_x=0.01; S_y=0.47)	−12.4
4.94	0.003 (S_z=0.02)	0.1
5.13	0.002 (S_x=0.02; S_y=0.002)	1.7
5.47	0.99 (S_x=7.1; S_y=0.38)	158.3
5.62	0.23 (S_x=0.83; S_y=0.85)	−165.6
	B3LYP	
3.72 (L_a)	0.049 (S_x=0.36; S_y=0.17)	14.4
4.17	0.002 (S_z=0.02)	1.2
4.36 (L_b)	0.015 (S_x=0.1; S_y=0.03)	−7.9
4.71	0.003 (S_z=0.03)	0.9
4.90	0.03 (S_x=0.02; S_y=0.45)	1.2
5.29	0.95 (S_x=7.1; S_y=0.1)	160.7
5.40	0.14 (S_x=0.74; S_y=0.18)	−149.1
	CAM-B3LYP	
3.99 (L_a)	0.05 (S_x=0.14; S_y=0.09)	14.0
4.53	0.003 (S_z=0.03)	0.7
4.59 (L_b)	0.03 (S_x=0.14; S_y=0.08)	−13.5
4.72	0.002(S_z=0.02)	4.4
5.17	0.01 (S_x=0.22; S_y=0.001)	0.7
5.59	1.12 (S_x=8.1; S_y=0.17)	140.1
5.75	0.16 (S_x=0.56; S_y=0.60)	−129.0

Acknowledgement

S.C. acknowledges financial support from the Independent Research Fund Denmark—Natural Sciences, Research Project 2, grant no. 7014-00258B. S.G. thanks the University of Brescia and MIUR for a visiting grant under the auspices of the Doctorate program.

Supporting Information Available

Additional information: geometrical parameters of the optimized structures of naphthalene and its derivatives. Alternative renderings of the spectra.

References

(1) Schatz, P. N.; McCaffery, A. J. The Faraday effect. *Q. Rev. Chem. Soc.* **1969**, *23*, 552–584.

(2) Foss, J. G.; McCarville, M. E. MCD of Simple and Catacondensed Aromatics. *J. Chem. Phys.* **1966**, *44*, 4350–4351.

(3) Foss, J. G.; McCarville, M. E. Some Generalizations Concerning the Magnetic Circular Dichroism of Substituted Benzenes. *J. Am. Chem. Soc.* **1967**, *89*, 30–32.

(4) Stephens, P. J.; Schatz, P. N.; Ritchie, A. B.; McCaffery, A. J. Magnetic Circular Dichroism of Benzene, Triphenylene, and Coronene. *J. Chem. Phys.* **1968**, *48*, 132–138.

(5) Larkindale, J. P.; Simkin, D. J. Magnetic Circular Dichroism of Benzene, Triphenylene, and Coronene. *J. Chem. Phys.* **1971**, *55*, 5668–5674.

(6) Michl, J. Magnetic circular dichroism of cyclic π-electron systems. 1. Algebraic solution of the perimeter model for the A and B terms of high-symmetry systems with a (4N+2)-electron [n]annulene perimeter. *J. Am. Chem. Soc.* **1978**, *100*, 6801–6811.

(7) Michl, J. Magnetic circular dichroism of cyclic π-electron systems. 2. Algebraic solution of the perimeter model for the B terms of systems with a (4N + 2)-electron [n]annulene perimeter. *J. Am. Chem. Soc.* **1978**, *100*, 6812–6818.

(8) Michl, J. Magnetic circular dichroism of cyclic π-electron systems. 3. Classification of cyclic π chromophores with a (4N + 2)-electron [n]annulene perimeter and general rules for substituent effects on the MCD spectra of soft chromophores. *J. Am. Chem. Soc.* **1978**, *100*, 6819–6824.

(9) Platt, J. R. Classification of Spectra of Cata-Condensed Hydrocarbons. *J. Chem. Phys.* **1949**, *17*, 484–49.

(10) Whipple, M. R.; Vasak, M.; Michl, J. Magnetic circular dichroism of cyclic π-electron systems. 8. Derivatives of naphthalene. *J. Am. Chem. Soc.* **1978**, *100*, 6844–6852.

(11) Grimme, S.; Parac, M. Substantial Errors from Time-Dependent Density Functional Theory for the Calculation of Excited States of Large π Systems. *ChemPhysChem* **2003**, *4*, 292–295.

(12) Parac, M.; Grimme, S. A TDDFT study of the lowest excitation energies of polycyclic aromatic hydrocarbons. *Chem. Phys.* **2003**, *292*, 11–21.

(13) Krykunov, M.; Grimme, S.; Ziegler, T. Accurate Theoretical Description of the $^1\mathrm{L}_a$ and $^1\mathrm{L}_b$ Excited States in Acenes Using the All Order Constricted Variational Density Functional Theory Method and the Local Density Approximation. *J. Chem. Theory Comput.* **2012**, *8*, 4434–4440.

(14) Richard, R. M.; Herbert, J. M. Time-Dependent Density-Functional Description of the ^1L_a State in Polycyclic Aromatic Hydrocarbons: Charge-Transfer Character in Disguise? *J. Chem. Theory Comput.* **2011**, *7*, 1296–1306.

(15) Acharya, A.; Chaudhuri, S.; Batista, V. S. Can TDDFT Describe Excited Electronic States of Naphthol Photoacids? A Closer Look with EOM-CCSD. *J. Chem. Theory Comput.* **2018**, *14*, 867–876.

(16) Khani, S. K.; Faber, R.; Santoro, F.; Hättig, C.; Coriani, S. UV Absorption and Magnetic Circular Dichroism Spectra of Purine, Adenine, and Guanine: A Coupled Cluster Study in Vacuo and in Aqueous Solution. *J. Chem. Theory Comput.* **2019**, *15*, 1242–1254.

(17) Kendall, R. A.; Dunning, T. H.; Harrison, R. J. Electron affinities of the first-row atoms revisited. Systematic basis sets and wave functions. *J. Chem. Phys.* **1992**, *96*, 6796–6806.

(18) Coriani, S.; Jørgensen, P.; Ruud, K.; Rizzo, A.; Olsen, J. Ab Initio Determinations of Magnetic Circular Dichroism. *Chem. Phys. Lett.* **1999**, *300*, 61–68.

(19) Coriani, S.; Hättig, C.; Jørgensen, P.; Helgaker, T. Gauge-origin independent magneto-optical activity within coupled cluster response theory. *J. Chem. Phys.* **2000**, *113*, 3561.

(20) Kjærgaard, T.; Coriani, S.; Ruud, K. Ab initio calculation of magnetic circular dichroism. *Wiley Interdisciplinary Reviews: Computational Molecular Science* **2012**, *2*, 443–455.

(21) Faber, R.; Ghidinelli, S.; Hättig, C.; Coriani, S. Magnetic circular dichroism spectra from resonant and damped coupled cluster response theory. *J. Chem. Phys.* **2020**, *153*, 114105.

(22) Furche, F.; Ahlrichs, R.; Hättig, C.; Klopper, W.; Sierka, M.; Weigend, F. *WIREs Computational Molecular Science* **2014**, *4*, 91–100.

(23) Balasubramani, S. G.; Chen, G. P.; Coriani, S.; Diedenhofen, M.; Frank, M. S.; Franzke, Y. J.; Furche, F.; Grotjahn, R.; Harding, M. E.; Hättig, C.; Hellweg, A.; Helmich-Paris, B.; Holzer, C.; Huniar, U.; Kaupp, M.; Marefat Khah, A.; Karbalaei Khani, S.; Mller, T.; Mack, F.; Nguyen, B. D.; Parker, S. M.; Perlt, E.; Rappoport, D.; Reiter, K.; Roy, S. et al. TURBOMOLE: Modular program suite for ab initio quantum-chemical and condensed-matter simulations. *J. Chem. Phys.* **2020**, *152*, 184107.

(24) Weigend, F.; Köhn, A.; Hättig, C. Efficient use of the correlation consistent basis sets in resolution of the identity MP2 calculations. *J. Chem. Phys.* **2001**, *116*, 3175–3183.

(25) Solheim, H.; Frediani, L.; Ruud, K.; Coriani, S. An IEF-PCM Study of Solvent Effects on the Faraday B Term of MCD. *Theor. Chem. Accounts* **2008**, *119*, 231–244.

(26) Kjærgaard, T.; Jørgensen, P.; Thorvaldsen, A. J.; Sałek, P.; Coriani, S. Gauge-origin Independent Formulation and Implementation of Magneto-Optical Activity within Atomic-Orbital-Density Based Hartree-Fock and Kohn-Sham Response Theories. *J. Chem. Theory Comp.* **2009**, *5*, 1997–2020.

(27) Becke, A. D. Density-functional thermochemistry. III. The role of exact exchange. *J. Chem. Phys.* **1993**, *98*, 5648–52.

(28) Yanai, T.; Tew, D. P.; Handy, N. C. A new hybrid exchangecorrelation functional using the Coulomb-attenuating method (CAM-B3LYP). *Chem. Phys. Lett.* **2004**, *393*, 51–57.

(29) Aidas, K.; Angeli, C.; Bak, K. L.; Bakken, V.; Bast, R.; Boman, L.; Christiansen, O.; Cimiraglia, R.; Coriani, S.; Dahle, P.; Dalskov, E. K.; Ekström, U.; Enevoldsen, T.; Eriksen, J. J.; Ettenhuber, P.; Fernández, B.; Ferrighi, L.; Fliegl, H.; Frediani, L.; Hald, K.; Halkier, A.; Hättig, C.; Heiberg, H.; Helgaker, T.; Hennum, A. C. et al. The Dalton Quantum Chemistry Program System. *WIREs Comput. Mol. Sci.* **2014**, *4*, 269.

(30) Fahleson, T.; Kauczor, J.; Norman, P.; Santoro, F.; Improta, R.; Coriani, S. TD-DFT Investigation of the Magnetic Circular Dichroism Spectra of Some Purine and Pyrimidine Bases of Nucleic Acids. *J. Phys. Chem. A* **2015**, *119*, 5476–5489.

(31) Quintessa, Graph Grabber 2.0. `https://www.quintessa.org/software/downloads-and-demos/graph-grabber-2.0`, (accessed: 11.01.2020).

(32) Hashimoto, T.; Nakano, H.; Hirao, K. Theoretical study of the valence $\pi \rightarrow \pi^*$ excited states of polyacenes: Benzene and naphthalene. *J. Chem. Phys.* **1996**, *104*, 6244–6258.

(33) Zilberg, S.; Haas, Y.; Shaik, S. Electronic Spectrum of Anthracene: An ab-initio Molecular Orbital Calculation Combined with a Valence Bond Interpretation. *J. Phys. Chem.* **1995**, *99*, 16558–16565.

(34) Wong, B. M.; Hsieh, T. H. Optoelectronic and Excitonic Properties of Oligoacenes: Substantial Improvements from Range-Separated Time-Dependent Density Functional Theory. *J. Chem. Theory Comput.* **2010**, *6*, 37043712.

(35) Vasak, M.; Whipple, M. R.; Michl, J. Magnetic circular dichroism of cyclic π-electron systems. 7. Aza analogs of naphthalene. *J. Am. Chem. Soc.* **1978**, *100*, 6838–6843.

(36) Andrews, L.; Kelsall, B. J.; Blankenship, T. A. Vibronic absorption spectra of naphthalene and substituted naphthalene cations in solid argon. *J. Phys. Chem.* **1982**, *86*, 2916–2926.

(37) Wessel, J.; McClure, D. Vibronic interactions in the naphthalene molecule. *Mol. Cryst. Liq. Cryst.* **1980**, *58*, 433–465.

(38) Kaminský, J.; Chalupský, J.; Štěpánek, P.; Kríz, J.; Bouř, P. Vibrational Structure in Magnetic Circular Dichroism Spectra of Polycyclic Aromatic Hydrocarbons. *J. Phys. Chem. A* **2017**, *121*, 9064–9073.

(39) Baba, H.; Suzuki, S. Electronic Spectra of Substituted Aromatic Hydrocarbons. II. Naphthols and Naphthylamines. *Bull. Chem. Soc. Jpn.* **1961**, *34*, 82–251.

(40) Suzuki, S.; Fujii, T.; Baba, H. Interpretation of electronic spectra by configuration analysis: Absorption spectra of monosubstituted naphthalenes. *J. Mol. Spectrosc.* **1973**, *47*, 243–251.

(41) Biermann, D.; Schmidt, W. Diels-Alder reactivity of polycyclic aromatic hydrocarbons. 1. Acenes and benzologs. *J. Am. Chem. Soc.* **1980**, *102*, 3163–3173.

(42) Messina, F.; Prémont-Schwarz, M.; Braem, O.; Xiao, D.; Batista, V. S.; Nibbering, E. T.; Chergui, M. Ultrafast Solvent-Assisted Electronic Level Crossing in 1-Naphthol. *Angew. Chem., Int. Ed.* **2013**, *27*, 6871–6875.

(43) Xiao, D.; Prémont-Schwarz, M.; Nibbering, E. T. J.; Batista., V. S. Ultrafast vibrational frequency shifts induced by electronic excitations: Naphthols in low dielectric media. *J. Phys. Chem. A* **2012**, *116*, 2775–2790.

(44) George, G. A.; Morris, G. C. The intensity of absorption of naphthalene from 30 000 cm^{-1} to 53 000 cm^{-1}. *J. Mol. Spectrosc.* **1968**, *26*, 67–71.

(45) Handa, T. The Interpretation of Absorption Spectra of Condensed Polycyclic Aromatic Hydrocarbons by Using a Simple Resonance Theory. I. The Resonance Structure of the Excited State in Correlation with Platts Theory. *Bull. Chem. Soc. Jpn.* **1963**, *36*, 235–247.

(46) Tajiri, A.; Hatano, M. MCD studies of azulene and naphthalene. *Chem. Phys. Lett.* **1975**, *34*, 29–33.

(47) Nakai, Y.; Mori, T.; Inoue, Y. Theoretical and Experimental Studies on Circular Dichroism of Carbo[N]Helicenes. *J. Phys. Chem. A.* **2012**, *116*, 7372–7385.

(48) Schreiber, M.; Silva-Junior, M. R.; Sauer, S. P. A.; Thiel, W. Benchmarks for Electronically Excited States: CASPT2, CC2, CCSD, and CC3. *J. Phys. Chem. A.* **2008**, *128*, 7372–7385.

(49) Santoro, F.; Improta, R.; Fahleson, T.; Kauczor, J.; Norman, P.; Coriani, S. Relative Stability of the L_a and L_b Excited States in Adenine and Guanine: Direct Evidence from TD-DFT Calculations of MCD Spectra. *J. Phys. Chem. Lett.* **2014**, *5*, 1806–1811.

(50) Wells, P. R.; Ehrenson, S.; Taft., R. W. Substituent Effects in the Naphthalene Series. An Analysis of Polar and Pi Delocalization Effects. *Prog. Phys. Org. Chem.* **1968**, *6*, 147–322.

(51) Krygowski, T. M.; Stepień, B. T. Sigma- and Pi-Electron Delocalization: Focus on Substituent Effects. *Chem. Rev.* **2005**, *105*, 3482–3512.

(52) Mohajeri, A.; Shahamirian, M. Substituent effect on local aromaticity in mono and di-substituted heterocyclic analogs of naphthalene. *J. Phys. Org. Chem.* **2010**, *23*, 440–450.

(53) Tichy, M.; Zahradnik, R. Physical properties and chemical reactivity of alternant hydrocarbons and related compounds. XVII. Electronic spectra of amino and hydroxy derivatives of benzenoid hydrocarbons. *J. Phys. Chem.* **1969**, *73*, 534–544.

(54) Ingold., C. Principles of an Electronic Theory of Organic Reactions. *Chem. Rev.* **1934**, *15*, 225–274.

(55) Lyle, S. M.; Lim, E. C. Polarization of singlet-singlet electronic transitions in substituted naphthalenes. *Chem. Phys. Lett.* **1972**, *17*, 367–369.

(56) Suzuki, S.; Fujii, T.; Ishikawa, T. Interpretation of electronic spectra by configuration analysis: Absorption spectra of monosubstituted naphthalenes with an electron-accepting group. *J. Mol. Spectrosc.* **1975**, *57*, 490–499.

Graphical TOC Entry